

Energetic Components of Cooperative Protein Folding

Hüseyin KAYA and Hue Sun CHAN

Department of Biochemistry, and

Department of Medical Genetics & Microbiology

Faculty of Medicine, University of Toronto

Toronto, Ontario M5S 1A8, Canada

Abstract

A new lattice protein model with a four-helix bundle ground state is analyzed by a parameter-space Monte Carlo histogram technique to evaluate the effects of an extensive variety of model potentials on folding thermodynamics. Cooperative helical formation and contact energies based on a 5-letter alphabet are found to be insufficient to satisfy calorimetric and other experimental criteria for two-state folding. Such proteinlike behaviors are predicted, however, by models with polypeptide-like local conformational restrictions and environment-dependent hydrogen bonding-like interactions.

PACS Numbers: 87.15.Aa, 87.15.Cc, 87.15.He, 87.15.By

Proteins are complex systems. Insight into their behaviors has been gained by simplified models of generic proteins [1-6]. To serve as stepping stones towards an elucidation of the physics of real proteins, however, these models must be subjected to rigorous evaluations against experiments. Recently, we found that a number of popular lattice protein models with 2, 3, and 20 residue types and pairwise additive contact energies do not satisfy the experimental criteria for two-state thermodynamic cooperativity which, among other conditions, requires a protein's van't Hoff to calorimetric enthalpy ratio $\Delta H_{\text{vH}}/\Delta H_{\text{cal}} \approx 1$ [7,8]. While certain G \bar{o} models are cooperative, they do not address the physical nature of protein interactions since their potentials are *teleological* [8] in the sense that the energetic favorability of the native conformation as a whole is presupposed.

It has since been proposed that a cooperative interplay between local conformational preferences and nonlocal interactions could give rise to proteinlike thermodynamics [7]. To evaluate the viability of this scenario, we introduce in this Letter a 55-mer chain model with a four-helix bundle ground state (Fig. 1) that shares common features with the corresponding protein motif [9]. The cubic-lattice helices are right-handed (called type (i) in Ref. [2]), as are most α -helices. The model has the following energetic components. (In the analysis below all energies are dimensionless and temperature independent.)

Contact energies. A reduced 5-letter alphabet (Fig. 1) identical to the one recently optimized [5] is used for nearest-neighbor interactions, with energy parameters from Table III of Kolinski et al. [10]. While these energies are proteinlike to some extent because hydrophobic groups are placed in the native core (Fig. 1), they do not represent the full interactions between amino acid residues [10]. Here they are adopted to capture heterogeneous aspects of intraprotein interactions [11].

Unfavorable local conformations. Two types of local non-proteinlike bond geometries are discouraged: the initiation of a left-handed (lh) helix (Fig. 2a), and one end of a helix taking a sharp turn (st) to fold back onto itself (Fig. 2b) are assigned unfavorable (> 0) energies to take into account that in real proteins left-handed α -helices are sterically disfavored, and that polypeptides are stiffer than a fully flexible chain [12].

Environment-dependent hydrogen bonding. The favorable many-body interactions ($\mathcal{E}_{\text{Hb}} < 0$) in Fig. 2c,d are introduced to explore an idea, suggested by experiments [13], that the collective strength of hydrogen bonds is stronger when they are buried in the core of a protein than when they are exposed to water. Hence we focus mainly on $b > 1$ cases below. Analogous interactions have been used before [7,14].

Cooperative helical propagation. An extra favorable energy is assigned to every two consecutive helical turns (Fig. 2e) to encourage helix elongation. Such an effect may arise from dipole-dipole interactions between amide groups in real α -helices [12].

The total energy of a conformation from these contributions is

$$E = E_{\text{contact}} + \gamma_{\text{lh}}N_{\text{lh}} + \gamma_{\text{st}}N_{\text{st}} + \mathcal{E}_{\text{Hb}}N_{\text{Hb}}^{(6)} + b\mathcal{E}_{\text{Hb}}N_{\text{Hb}}^{(8)} + \mathcal{E}_{\text{Helix}}N_{\text{Helix}} , \quad (1)$$

where E_{contact} is the sum of 5-letter contact energies, N_{lh} and N_{st} are respectively the numbers of all incidences of Fig. 2a,b. In the present analysis, N_{Helix} only counts those helices (Fig. 2e) that are parts of the four helices in the ground-state conformations (monomers 1–12, 15–26, 30–41, and 44–55; see Fig. 1); and the hydrogen bonding pairs counted by $N_{\text{Hb}}^{(6)}$ (Fig. 2c) and $N_{\text{Hb}}^{(8)}$ (Fig. 2d) are the 36 $(i, i + 3)$ or $(i, i + 5)$ contacting monomer pairs in the native helices. A first-principle treatment would have assigned hydrogen bonds and helical segments in a manner that do not require knowledge of the native structure. However, progress can nonetheless be made by the approach taken here, which seeks, as a first step in the inquiry, to ascertain the consequence of presupposing *local* native preferences, a presupposition that is notably less dependent on *a priori* knowledge than the assumption of *global* native preference in $\text{G}\bar{\text{o}}$ potentials.

To efficiently determine how thermodynamic properties vary with the model energetic parameters, we use a generalization [3,15] of the standard Metropolis Monte Carlo histogram technique [8,16] to eliminate the need to perform separate direct simulations for every parameter set of interest. Typical simulations are carried out with $\mathcal{E}_{\text{Hb}} = \mathcal{E}_{\text{Helix}} = 0$ at a certain temperature T' , during which numbers P of sampled conformations are binned into a multiple-dimensional array (histogram) according to $(E', N_{\text{Hb}}^{(6)}, N_{\text{Hb}}^{(8)}, N_{\text{Helix}})$, where

E' is the energy of the conformation. Thus the density of states of the simulated system $g(E', N_{\text{Hb}}^{(6)}, N_{\text{Hb}}^{(8)}, N_{\text{Helix}}) = P(E', N_{\text{Hb}}^{(6)}, N_{\text{Hb}}^{(8)}, N_{\text{Helix}})e^{E'/k_B T'}$, where k_B is Boltzmann's constant. It follows that the partition function for any \mathcal{E}_{Hb} , $\mathcal{E}_{\text{Helix}}$ at any temperature T is given by $\sum g(E', N_{\text{Hb}}^{(6)}, N_{\text{Hb}}^{(8)}, N_{\text{Helix}})e^{-E/k_B T}$, where the summation is over E' , $N_{\text{Hb}}^{(6)}$, $N_{\text{Hb}}^{(8)}$, and N_{Helix} , and $E = E' + \mathcal{E}_{\text{Hb}}(N_{\text{Hb}}^{(6)} + bN_{\text{Hb}}^{(8)}) + \mathcal{E}_{\text{Helix}}N_{\text{Helix}}$. A similar procedure is used to study the effects of γ_{lh} and γ_{st} .

Each Monte Carlo run consists of 1.53×10^9 attempted moves, the first 3×10^7 of which are excluded from data acquisition. To generate a multiple-dimensional histogram, a total of 20 runs at 10 different simulation T' s (around the transition region) are performed, with two different random initial conformations for each T' . Values of κ_2 estimated from different T' s agree well, with standard deviation $\approx 4\%$. We have conducted extensive comparisons with direct simulations to validate the method [17]. No energy lower than that of the structure in Fig. 1 has been encountered.

As in experimental calorimetry [18], we characterize the thermodynamic cooperativity of a model protein by its specific heat capacity C_P and $\Delta H_{\text{vH}}/\Delta H_{\text{cal}}$. When baseline subtraction is not applied to the C_P function, $\Delta H_{\text{vH}}/\Delta H_{\text{cal}}$ may be equated to $\kappa_2 \equiv 2T_{\text{max}}\sqrt{k_B C_P(T_{\text{max}})}/\Delta H_{\text{cal}}$, where $\Delta H_{\text{cal}} = \int_0^\infty dT C_P(T)$ is the calorimetric enthalpy, and $C_P(T)$ is maximum at $T = T_{\text{max}}$ [8]. Baseline subtractions amount to defining a multi-conformation native state and ignoring a part of the enthalpic variation in the denatured ensemble. This effectively reduces both the calorimetric enthalpy and the maximum heat capacity value, resulting in a modified enthalpy ratio $\kappa_2^{(s)}$ ($> \kappa_2$) [8].

Our main findings are summarized in Figs. 3 and 4. The apparent $\Delta H_{\text{vH}}/\Delta H_{\text{cal}} = \kappa_2^{(s)}$ after empirical baseline subtractions can often be close or equal to unity even when κ_2 is low (Fig. 4). However, as is the case for a 3-letter model, a large discrepancy between κ_2 and $\kappa_2^{(s)}$ is often symptomatic of non-proteinlike significant post-denaturational chain expansion at $T \gg T_{\text{max}}$ [8]. Therefore, for model evaluation, proteinlike thermodynamic cooperativity requires *both* a small $\kappa_2^{(s)} - \kappa_2$ and $\kappa_2^{(s)} \approx 1$.

Fig. 3 compares three models by this criterion. The least cooperative is a flexible chain

model with only pairwise additive contact energies. A second model with polypeptide-like local sterics has slightly enhanced cooperativity because populations of nonnative conformations with non-proteinlike local geometries that are hitherto favorable in a fully flexible chain model are reduced. However, both of these models are not proteinlike because of their significant post-denaturational chain expansions, as is evident from their thick denatured C_P “tails” at $T \gg T_{\max}$ (Fig. 3), which account for these models’ relatively large differences between $\kappa_2^{(s)}$ and κ_2 [8]. On the other hand, the model that also incorporates environment-dependent hydrogen bonding has more proteinlike thermodynamics: Its native C_P tail at $T \ll T_{\max}$ is thin, with C_P values lower on average than that of its denatured tail (Fig. 3). This implies that its native conformational diversity is limited, thus conforming better to NMR data [19] than a previously considered 20-letter model [8]. As for real proteins [20], its average radius of gyration undergoes a sharp change around T_{\max} , but has no appreciable post-denaturational increase (data not shown).

Fig. 4 surveys a range of energetic parameters. Remarkably, local helical cooperativity has only a small impact on overall folding cooperativity, and proteinlike thermodynamics is possible at $\mathcal{E}_{\text{Helix}} = 0$. While $\mathcal{E}_{\text{Helix}} < 0$ stabilizes the native state, it also stabilizes denatured conformations with partially intact native helices. Therefore, its effect on calorimetric cooperativity is not substantial because it cannot widen the average enthalpy difference between native and denatured states significantly [7,8]. In contrast, calorimetric cooperativity increases sharply with more negative \mathcal{E}_{Hb} . For $0.5 \leq b \leq 1.5$, this effect is not very sensitive to b . For example, $\mathcal{E}_{\text{Hb}} = -0.5$, $\mathcal{E}_{\text{Helix}} = 0$, $b = 0.5$ (and $\gamma_{\text{lh}} = 6.0$, $\gamma_{\text{st}} = 5.0$) lead to κ_2 , $\kappa_2^{(s)} = 0.85, 0.99$, which are only slightly lower than the κ_2 , $\kappa_2^{(s)}$ values of 0.90, 1.0 for the same \mathcal{E}_{Hb} and $\mathcal{E}_{\text{Helix}}$ in Fig. 4 for $b = 1.5$.

In addition, we found that a lattice version of helix capping [21] has a slight attenuating effect on cooperativity [17]. Consistent with experiments [22], in our model, tertiary interactions are essential in stabilizing helices in native structures. When folded independently, the two 12-mer sequences for the native helices at 1–12 and 15–26 are much less stable ($T_{\max} \sim 0.3$), and their thermal transitions are not calorimetrically cooperative.

Figs. 3 and 4 suggest that a cooperative interplay between local conformational preferences and nonlocal contact interactions, as exemplified by the environment-dependent hydrogen bonding in the model, is a viable mechanism for proteinlike thermodynamics; and that the required cooperative effect ($b\mathcal{E}_{\text{Hb}} = -0.8$) need not be exceedingly strong relative to the pairwise contact energies (average magnitude = 0.66). This observation is consistent with a previous high-coordination lattice model study [23], though the latter did not address the calorimetric criterion. The present approach did not consider non-native hydrogen bonding. Cooperativity in the present model would be reduced if such non-native conformations are favored. Further investigations using continuum models with polypeptide chain geometry are necessary to ascertain whether real proteins can have substantial number of non-native hydrogen bonds. While the present model should be regarded as tentative because it relies on local native information, its proteinlike features do not follow trivially from part of its interactions' native-centric nature *per se*. Important physical principles have emerged from our analysis because not all native-centric interaction schemes can bring about comparable enhancements in thermodynamic cooperativity: (i) The fact that $\mathcal{E}_{\text{Helix}} < 0$ is neither necessary nor sufficient for proteinlike thermodynamics suggests that multi-body interactions that favors local native conformation irrespective of tertiary packing cannot account for calorimetric cooperativity. (ii) A $G\bar{o}$ model for the ground-state conformations in Fig. 1, which exploits both local and nonlocal native information but is based exclusively on pairwise additive interactions, has $\kappa_2 = 0.73$ and is thus less cooperative than the model with $\kappa_2 = 0.91$ in Fig. 3. (iii) Proteinlike steric effects contribute to cooperativity. If non-proteinlike local conformations were not disfavored in the latter model (i.e., if $\gamma_{\text{lh}} = \gamma_{\text{st}} = 0$), κ_2 would be reduced to 0.85.

We have thus mapped out a general investigative strategy and established the viability of a folding scenario. It should be emphasized, however, that satisfying the requirements for thermodynamic cooperativity is clearly necessary but not sufficient for the validity of a scenario's underlying physical mechanisms. Whether hydrogen bonding is favorable to native stability remains controversial [13,24]. The present choice of $\mathcal{E}_{\text{Hb}} < 0$ is motivated

by experiments [13]. But there have been theoretical suggestions that hydrogen bonding disfavors the folded state of a protein [24]. In the present modeling framework, that would be detrimental to calorimetric cooperativity as it corresponds to $\mathcal{E}_{\text{Hb}} > 0$, leading to κ_2 s even smaller than the $\mathcal{E}_{\text{Hb}} = 0$ case (Fig. 3). For instance, when $\mathcal{E}_{\text{Hb}} = +0.1$ and $\mathcal{E}_{\text{Helix}} = 0$, (and $\gamma_{\text{h}} = 6.0$, $\gamma_{\text{st}} = 5.0$), $\kappa_2, \kappa_2^{(\text{s})} = 0.51, 0.80$ for $b = 0.5$ and $\kappa_2, \kappa_2^{(\text{s})} = 0.45, 0.70$ for $b = 1.5$, respectively. If that turns out to be the case, there would be added impetus to extend the present method to ascertain the role of other mechanisms such as sidechain packing [4,8,25] in protein calorimetric two-state cooperativity.

This work was supported by Medical Research Council of Canada grant MT-15323.

REFERENCES

- [1] J. D. Bryngelson *et al.*, *Proteins: Struct. Funct. Genet.* **21**, 167 (1995); K. A. Dill *et al.*, *Protein Sci.* **4**, 561 (1995); H. Li *et al.*, *Science* **273**, 666 (1996); V.S. Pande, A. Yu. Grosberg, and T. Tanaka, *Biophys. J.* **73**, 3192 (1997); E.I. Shakhnovich, *Curr. Opin. Struct. Biol.* **7**, 29 (1997); H. S. Chan and K. A. Dill, *Proteins: Struct. Funct. Genet.* **30**, 2 (1998); C. Micheletti *et al.*, *Phys. Rev. Lett.* **82**, 3372 (1999).
- [2] H. S. Chan and K. A. Dill, *J. Chem. Phys.* **92**, 3118 (1990); **107**, 10353 (1997).
- [3] N.D. Socci and J.N. Onuchic, *J. Chem. Phys.* **103**, 4732 (1995).
- [4] D. K. Klimov, and D. Thirumalai, *Fold. Des.* **3**, 127 (1998).
- [5] J. Wang and W. Wang, *Nature Struct. Biol.* **6**, 1033 (1999).
- [6] H. S. Chan, *Nature (London)* **392**, 761 (1998).
- [7] H. S. Chan, *Proteins: Struct. Funct. Genet.* **40**, 543 (2000).
- [8] H. Kaya and H. S. Chan, *Proteins: Struct. Funct. Genet.* **40**, 637 (2000).
- [9] C. Branden and J. Tooze, *Introduction to Protein Structure* (Garland, New York, 1991).
- [10] A. Kolinski, A. Godzik, and J. Skolnick, *J. Chem. Phys.* **98**, 7420 (1993).
- [11] H. S. Chan and K. A. Dill, *Proteins: Struct. Funct. Genet.* **24**, 335 (1996); P. G. Wolynes, *Nature Struct. Biol.* **4**, 871 (1997); H. S. Chan, *Nature Struct. Biol.* **6**, 994 (1999).
- [12] C. R. Cantor and P. R. Schimmel, *Biophysical Chemistry* (Freeman, San Francisco, 1980).
- [13] S. M. Habermann and K. P. Murphy, *Protein Sci.* **5**, 1229 (1996); J. K. Myers and C. N. Pace, *Biophys. J.* **71**, 2033 (1996).
- [14] S. Takada, Z. Luthey-Schulten, and P. G. Wolynes, *J. Chem. Phys.* **110**, 11616 (1999).

- [15] J.-E. Shea *et al.*, J. Chem. Phys. **109**, 2895 (1998).
- [16] A. M. Ferrenberg and R. H. Swendsen, Phys. Rev. Lett. **63**, 1195 (1989).
- [17] H. Kaya and H. S. Chan, in preparation.
- [18] P. L. Privalov and S. A. Potekhin, Meth. Enzymol. **131**, 4 (1986); E. Freire, in *Protein Stability and Folding: Theory and Practice*, edited by B. A. Shirley, Methods in Molecular Biology, Vol. 40 (Humana, Totowa, New Jersey, 1995).
- [19] D. Yang *et al.*, J. Mol. Biol. **272**, 790 (1997).
- [20] T. R. Sosnick and J. Trehwella, Biochemistry **31**, 8329 (1992); Y. Hagihara *et al.*, Fold. Des. **3**, 195 (1998).
- [21] L. G. Presta and G. D. Rose, Science **240**, 1632 (1988); R. Aurora, R. Srinivasan, and G. D. Rose, Science **264**, 1126 (1994).
- [22] K. A. Dill, Biochemistry **29**, 7133 (1990).
- [23] A. Kolinski, W. Galazka, and J. Skolnick, Proteins: Struct. Funct. Genet. **26**, 271 (1996).
- [24] B. Honig and A.-S. Yang, Adv. Protein Chem. **46**, 27 (1995); N. Ben-Tal *et al.*, J. Phys. Chem. B **101**, 450 (1997).
- [25] E. I. Shakhnovich and A. V. Finkelstein, Biopolymers **28**, 1667 (1989); S. Bromberg and K. A. Dill, Protein Sci. **3**, 997 (1994).

Figure Captions

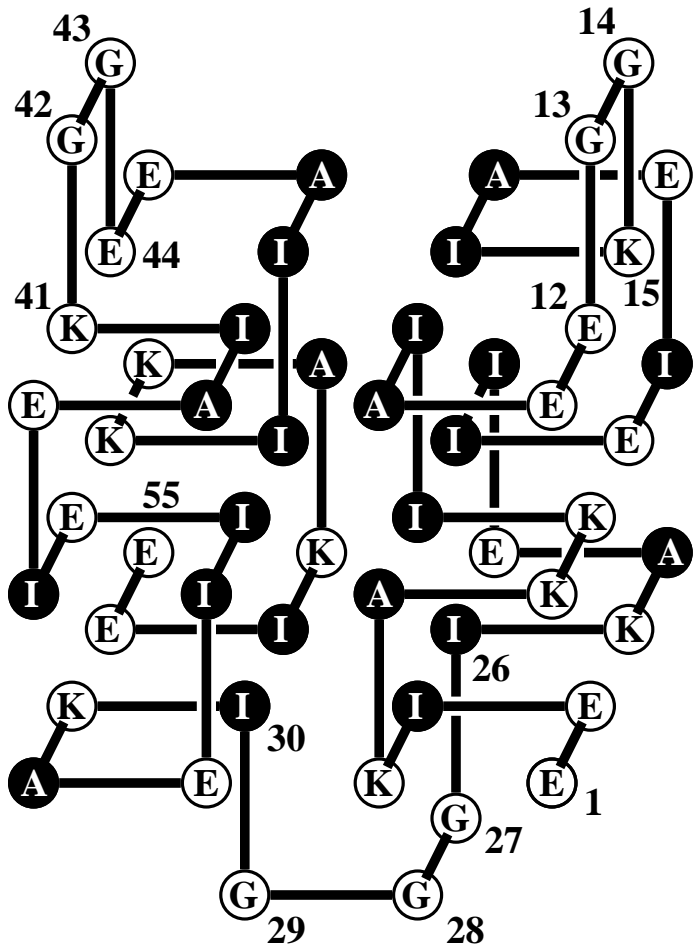
Fig. 1. Ground state conformations of the model. Black beads denote nominally hydrophobic monomers. The numbers label selected sequence positions. Each of the 3 short loops at positions (13, 14), (27, 28, 29), and (42, 43) has two iso-energetic local conformations. Thus the ground state has 8 conformations, one of which is shown.

Fig. 2. Energetic components of the model. (a,b) Each contact marked by a double arrow is assigned an energy (as shown). The dotted lines in (b) depict an alternate path of the chain from monomer $i - 3$ to i that has one instead of two unfavorable contacts. Similarly, an energy is associated with each buried hydrogen bond (c,d) and each occurrence of two consecutive turns (layers) of a right-handed lattice helix (e). In (c,d), hydrogen bonds are represented as ladders linking pairs of encircled monomers. Their burial requires occupation of at least 6 of their neighbor sites. The energy of a completely buried bond with 8 occupied neighbor sites (d) can be stronger ($b > 1$) or weaker ($b < 1$) than a partially buried bond with 6 or 7 occupied neighbor sites. The latter two cases have the same energy \mathcal{E}_{Hb} and are accounted for collectively by $N_{\text{Hb}}^{(6)}$ in Eq. (1).

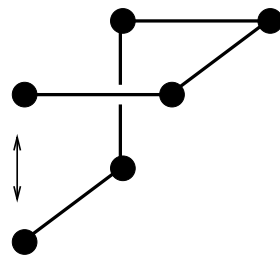
Fig. 3. Specific heat capacity functions. In all three cases shown, $\mathcal{E}_{\text{Helix}} = 0$. T_{max} s are marked by vertical lines. From left to right, the first model has only the 5-letter pairwise contact energies ($\gamma_{\text{lh}} = \gamma_{\text{st}} = \mathcal{E}_{\text{Hb}} = 0$). In addition to these, the second model incorporates the repulsive interactions in Fig. 2a,b, with $\gamma_{\text{lh}} = 6.0$ and $\gamma_{\text{st}} = 5.0$. The third model further adds the favorable hydrogen-bonding energies in Fig. 2c,d, with $\mathcal{E}_{\text{Hb}} = -0.53$, $b\mathcal{E}_{\text{Hb}} = -0.8$, and $b = 1.5$. $\kappa_2 = 0.55$, 0.62 , and 0.91 , and after the plotted inclined baselines are subtracted, $\kappa_2^{(s)} = 0.93$, 0.93 , and 1.01 , respectively.

Fig. 4. Calorimetric cooperativity as a function of local helical cooperativity and environment-dependent hydrogen bonding strength, with $b = 1.5$, $\gamma_{\text{lh}} = 6.0$ and $\gamma_{\text{st}} = 5.0$.

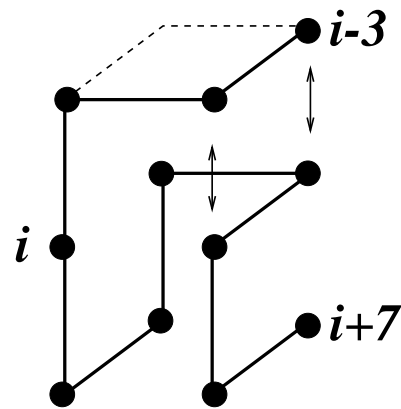
$\kappa_2^{(s)}$ and κ_2 are given by the upper and lower surfaces, respectively. The black dots connected by a vertical bar mark the parameters for the most cooperative case in Fig. 3. $\kappa_2^{(s)}$ are calculated using empirical baselines [8] constructed as tangents of the C_P function at $C_P''(T)/C_P''(T_{\max}) = -0.001$, where $C_P'' \equiv d^2C_P/dT^2$ (see Fig. 3).



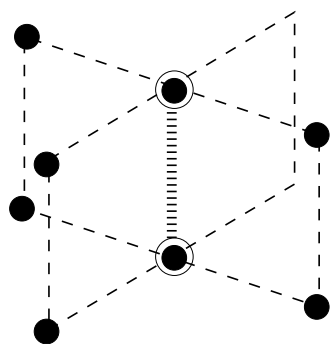
Kaya and Chan, Figure.1



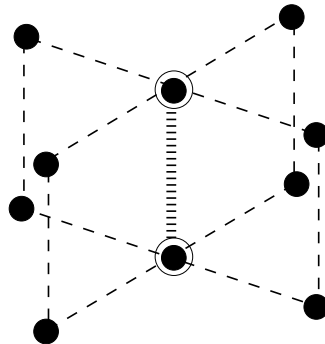
γ_{lh}
(a)



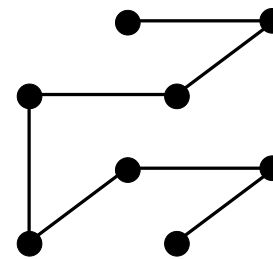
γ_{st}
(b)



\mathcal{E}_{Hb}
(c)

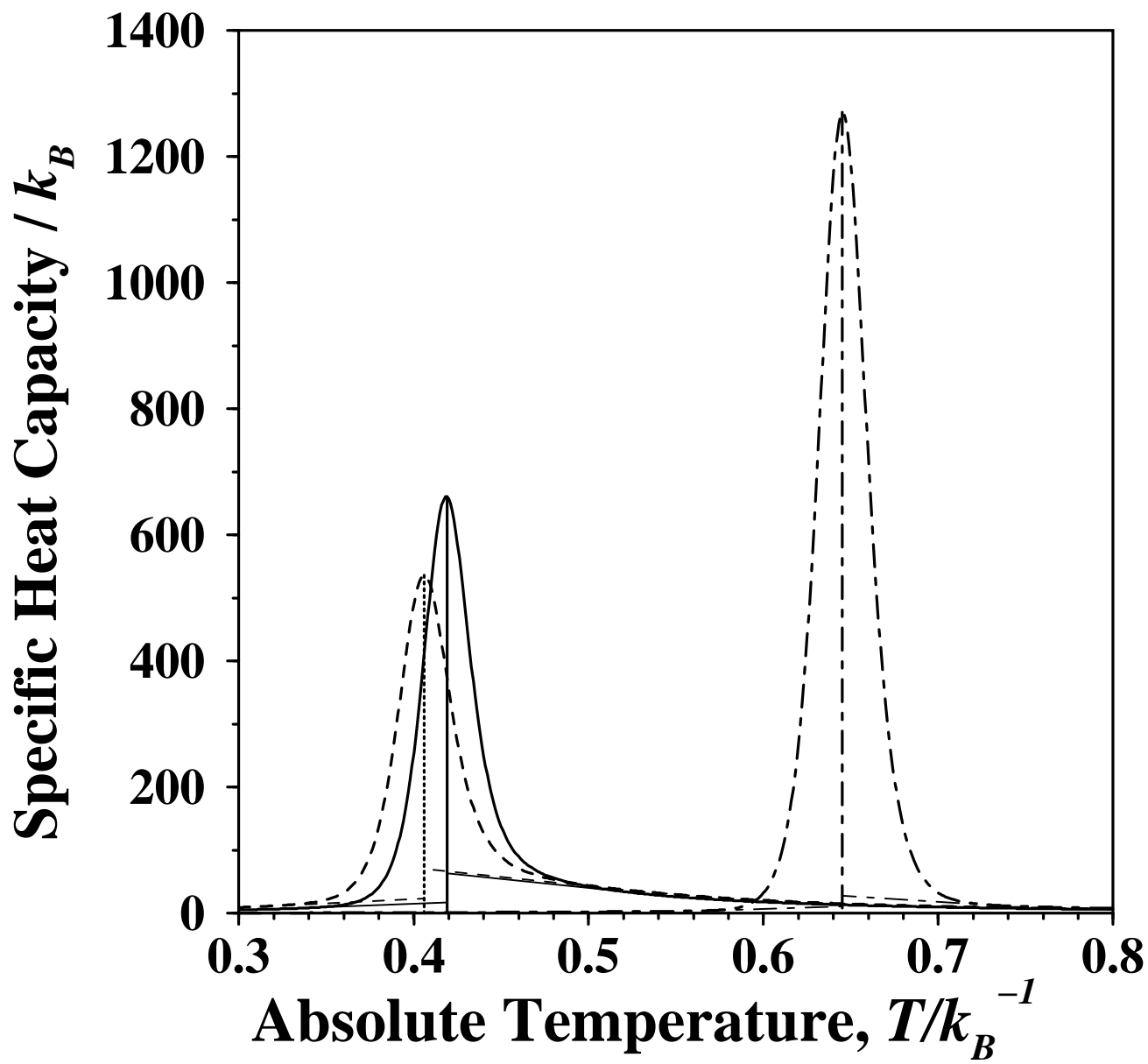


$b\mathcal{E}_{Hb}$
(d)

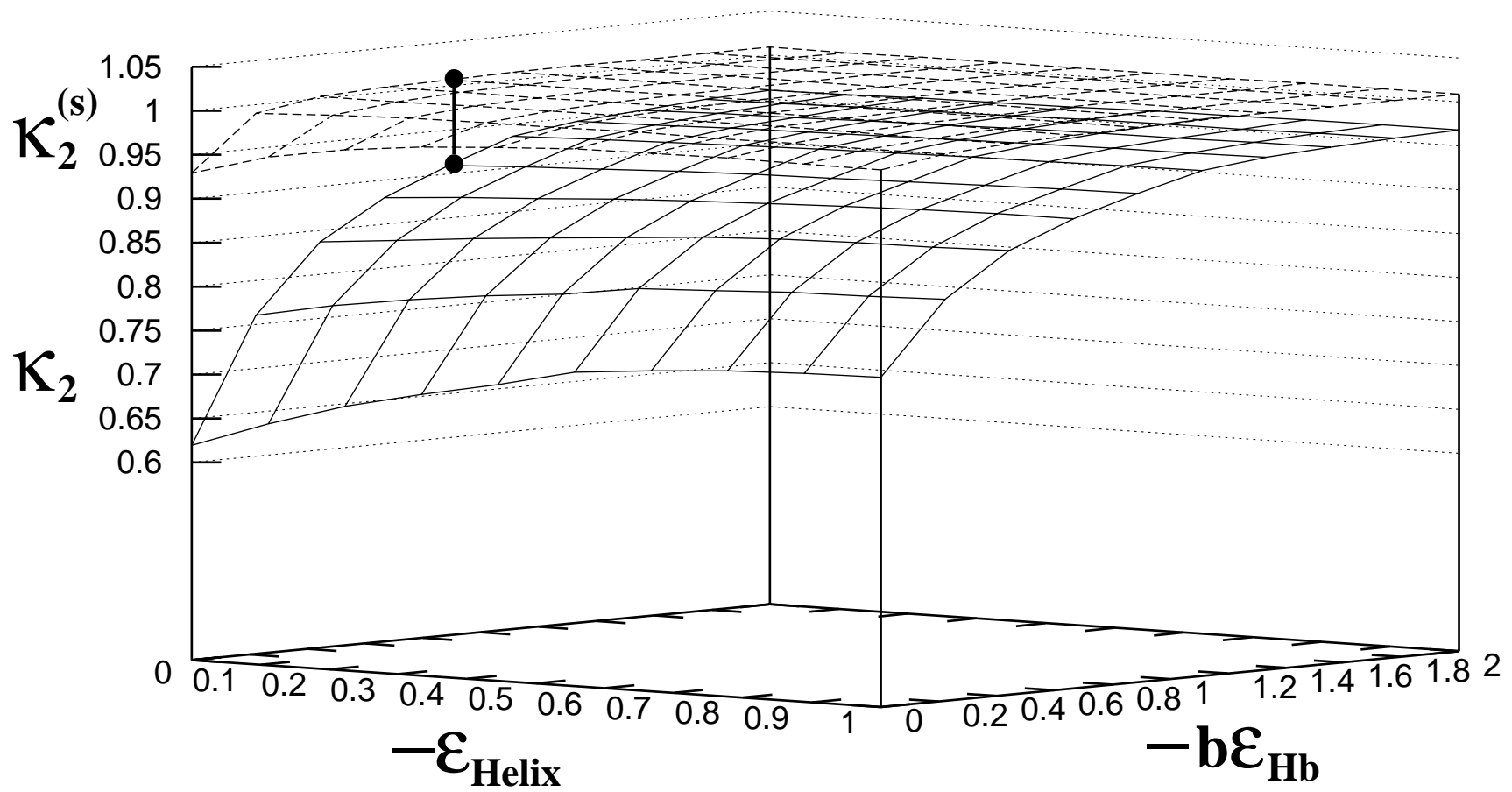


\mathcal{E}_{Helix}
(e)

Kaya and Chan, Figure.2



Kaya and Chan, Figure.3



Kaya and Chan, Figure.4